J Mater Sci (2006) 41:5712–5717
DOI 10.1007/s10853-006-0078-8

LETTER

Multiphase niobium aluminides fabricated via reaction synthesis

**E. J. Minay · I. Pong · H. B. McShane ·
R. D. Rawlings**

Received: 18 January 2006 / Accepted: 27 March 2006 / Published online: 27 May 2006

Niobium aluminides have been considered as a potential high temperature structural material [1–3]. They are expected to exhibit high elastic stiffness, strength and creep resistance at elevated temperatures. One of the notable advantages of niobium aluminides are the high melting points (which can be seen on the phase diagram in Fig. 1) compared to those of other, more commonly considered aluminide systems. Titanium and nickel alumindes are generally limited to structural applications below 1000 °C [5, 6], however, niobium aluminides can have extremely high strength even above 1200 °C and the incorporation of ductile reinforcements of metallic niobium can be used to lower the ductile to brittle transition temperatures and increase room temperature fracture toughness [1]. However, melting and casting of niobium aluminides presents several difficulties due to the high temperatures required, high evaporation rate of aluminium and the wide difference in the melting points and densities of niobium and aluminium. Homogeneity and composition control has presented particular difficulties and resulted in the development of specialised melting equipment [7]. Special mould materials are used due to the high casting temperatures required and high reactivity of the Nb–Al melt. Aluminium rich phases are particularly susceptible to microcracks occurring during casting and, despite the good high temperature properties, low ductility and toughness at room temperature make it a difficult material to machine. Reaction synthesis offers a potential solution to some of these processing difficulties. Advantages include: (i) the reduction in externally applied energy, as the heat of reaction is used to heat and soften or melt the intermetallics formed, (ii) short heating and cooling times, resulting in fine scale microstructures and reduced contamination from mould materials and the atmosphere, (iii) near net shape forming, thus reducing machining requirements, and (iv) the possibility of producing composites by incorporation of a second phase in the reacting mixture [8]. However reactive processing can result in relatively high levels of porosity, due to the initial density of the reacting powder compact, volume changes during reaction and Kirkendall porosity. Furthermore, the reaction can be difficult to control and may not go to completion; also loss of shape can occur due to melting, gas evolution and shrinking during densification. Subsequent and simultaneous application of pressure by hot forging or hot extrusion can be used to remove porosity from aluminides fabricated through reaction synthesis [9, 10]. This letter presents the results from a series of reaction synthesis trials across the Nb–Al system. In light of this the suitability of simultaneous application of pressure in order to densify the intermetallics formed is considered. Interesting fine scale microstructural features have been obtained.

Elemental aluminium powder (< 45 μm, 99.9%Al, ALPOCO, UK) and niobium powder (< 74 μm, 99.85%Nb, Goodfellow, UK) were mixed in the stoichiometric atomic ratios of 21Nb:4Al, 4Nb:1Al, 3Nb:1Al, 2Nb:1Al, 3Nb:2Al, 1Nb:1Al, 2Nb:3Al, 1Nb:3Al and 1Nb:4Al as marked by the lines on the phase diagram shown in Fig. 1. The dry powders were mixed in air, in a polypropylene bottle on a tubular mixer for 30 min. Samples of the mixed powders were cold compacted in a single ended steel die coated with zinc stearate powder under a pressure of 400 MPa that was applied for 5 s. After compaction the green pellets measured 8 mm in diameter and approximately 10 mm in height. The green density, determined from the geometry

E. J. Minay (✉) · I. Pong · H. B. McShane · R. D. Rawlings
Technology & Medicine, Imperial College of Science, Royal School of Mines, Prince Consort Road , London SW7 2BP, UK
e-mail: e.minay@ic.ac.uk

Fig. 1 Al–Nb phase diagram (from [4]), vertical lines represent the stoichiometry of the elemental mixture in the green compacts prior to heating

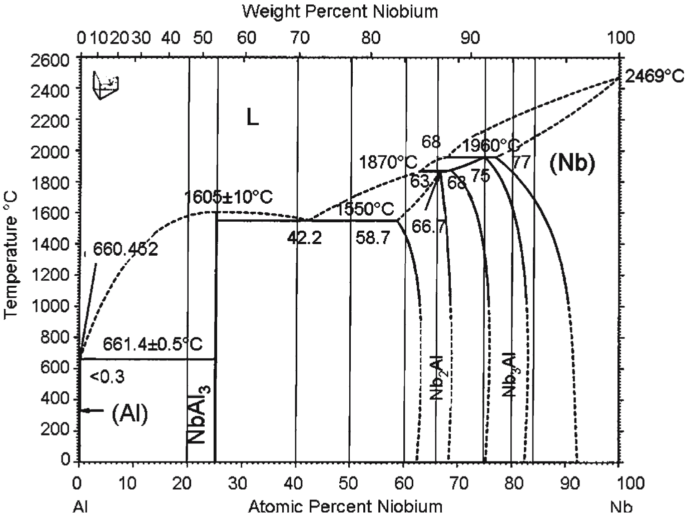

and mass of the pellets was between 89% and 96% in all cases. A small hole was drilled into each sample along the cylinder axis to enable a type-K thermocouple to be inserted approximately in the centre of the pellet. The pellets were placed in a hot alumina crucible in a pot furnace preheated to 750 °C. The temperature reading measured by the thermocouple was recorded using a chart recorder and for some samples the temperature was also measured using a hand held infrared pyrometer. An emissivity of 0.2 was assumed for all samples when calibrating the infrared pyrometer. Samples were removed from the pot furnace and immediately quenched in a large bucket of water at various stages during the reaction. Sections were cut from the quenched samples using a diamond impregnated saw and polished using wet SiC paper and diamond pastes down to 1 μm. The samples were examined using a JEOL LV5610 scanning electron microscope equipped with a backscattered detector and X-ray diffraction traces were recorded using a Phillips X-ray diffractometer, employing CuK_α radiation in conjunction with a PW 1050/25 model goiniometer calibrated against a Si standard {111} peak.

Figure 2 shows the temperature time profile, recorded using the thermocouple, for four of the pellet compositions. All of the samples reached 660 °C in approximately 1–2 min. At this temperature a plateau in the temperature time profile was observed. As the aluminium content increased so did the duration of this plateau. Similar behaviour has been observed previously in both this and other systems in which the melting point of aluminium is the lowest liquidus temperature [11–13]. During this plateau in temperature small globules of silvery liquid metal were observed to extrude from the pellet surface before being absorbed back into the pellet. Up to the plateau the temperature measured using the pyrometer lagged behind that of the thermocouple by approximately 40 °C. This may be due to an incorrect assumption in the value of the emissivity of the material, or due to the observed, top surface of the pellet being cooled due to the small opening in the lid of the pot furnace. Fol-

Fig. 2 Temperature time profiles of pellets mixed to the following stoichiometries: 3Nb:1Al, 2Nb:1Al, 1Nb:1Al and 1Nb:3Al. The melting point of aluminium is marked as a dashed line

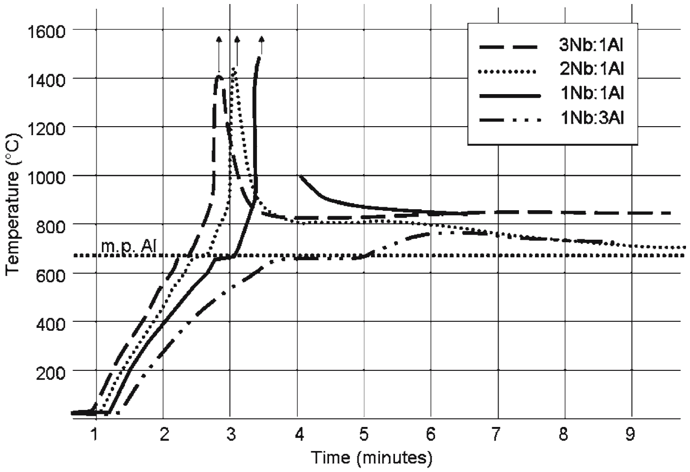

lowing the plateau the temperature of the pellets continued to rise. In the samples containing 75 atm% and greater of aluminium the rate of increase in temperature was gradual and the maximum temperature reached was relatively low, being below 900 °C. In contrast, in the samples containing 40 atm% and greater of niobium two stages were clearly apparent, a fast increase to around 900 °C (above the furnace temperature) followed by an even more rapid increase to over 1400 °C as the combustion reaction occurred. During those combustion reactions in which the pyrometer was used, the peak temperature measured by the pyrometer was higher by about 300 °C than that measured by the type K thermocouple. This is likely due to the temperatures rising above that which can be accurately measured by a type K thermocouple. In some cases the thermocouple broke or fell out of the sample during this reaction, but in those cases where the thermocouple remained intact and inside the sample the temperature recorded by the thermocouple and the pyrometer were again in reasonably close agreement as the sample cooled below 1400 °C. During cooling the pyrometer temperatures were generally 40 °C higher than those measured by the thermocouple (whereas on heating the pyrometer temperatures were 40 °C lower). This is most likely due to the exothermic oxidation of the surface of the pellets. Further evidence for the exothermic oxidation was observed in the niobium-rich samples where a second very shallow peak was observed following the highly exothermic reaction and the temperature remained around 850 °C for an extended period of time. During this time the surface of the pellet was observed to disintegrate into a pale green powder, which turned white as it cooled down.

The reacted pellets consisted of two distinct regions, a multiphase, niobium-rich centre surrounded by a more porous, multiphase aluminium-rich surface layer. These two regions were already apparent in samples quenched during the plateau at 660 °C. In samples quenched from this temperature the surface layer consisted of small niobium particles surrounded by a layer of $NbAl_3$. Globules of aluminium of about 1 mm diameter that had extruded from the original surface of the pellet were also observed. The centre of the pellet contained niobium particles surrounded by an aluminium matrix with a very thin interface layer of intermetallic phases between the aluminium matrix and the niobium particles. However, the amount of intermetallics present was small and no intermetallic phases were detected by X-ray diffraction (shown in Fig. 3a). The two regions are illustrated in Fig. 4a which shows a backscattered electron image of the 3Al:1Nb sample quenched during the plateau at 660 °C; the niobium is the bright phase towards the centre of the sample, at the edge a small amount light grey $NbAl_3$ is visible as well as darker aluminium, and the resin that the sample was mounted in is also visible to the far right of the micrograph. These observations support the initial step being melting of aluminium prior to the ignition of the combustion reaction. There is some disagreement in the literature as to whether all the aluminium melts prior to solid intermetallic phases precipitating out [12–15]. It is difficult to establish if all the aluminium melts during the plateau stage as the various techniques employed each have their limitations—intermetallics may form during the quenching in the type of experiments described here, whereas time resolved X-ray diffraction experiments pose difficulties in detecting small fractions of intermetallic phases and clearly distinguishing the phases present as many of the peaks are close to one another. Furthermore, usually the angular range and the time resolution possible make the study of the very rapid reactions difficult. Zhu et al. [14] have calculated that in the Ni–Al system only approximately one third of the aluminium melts during the plateau, however [13, 15] found aluminium melting to be complete in both the Ti–Al and Nb–Al systems. The layer of intermetallic phase surrounding the niobium particles would seem to suggest that the intermetallic exists prior to quenching, however it may have formed due to solid state reactions during heating rather than from reaction between liquid aluminium and solid niobium during the plateau. The current experiments show some evidence of a small amount of intermetallic forming due to solid state reactions both in the SEM images and also in the noticeable increase in gradient of the temperature time profiles beginning at around 600 °C, this was not observed previously in the synthesis of $NbAl_3$ [12, 13]. Occasionally initiation of the rapid and highly exothermic reactions to form intermetallic phases has been observed below the melting point of aluminium, but this can be attributed to exothermic, solid state reactions raising the local temperature to a point at or above the lowest liquidus temperature, a reduction in melting point of the aluminium powder due to impurities, nanoscale or severely deformed powders, or increases in temperature due to plastic deformation [16, 17]. Similarly higher reported initiation temperatures may be explained due to relatively slow kinetics and rapid heating rates.

Clearly if the first step of the reaction mechanism under these conditions is the complete melting of aluminium, which remains liquid for a significant period of time prior to the formation of intermetallic phases then some methods to reduce porosity by applying a pressure during the reaction will present problems. For example, during simultaneous heating and open-die forging the liquid formed is likely to be squeezed out of the reacting pellet by the applied pressure. Materials which react in this manner might be better processed by deformation subsequent to rather than simultaneously with the ignition of the exothermic reaction.

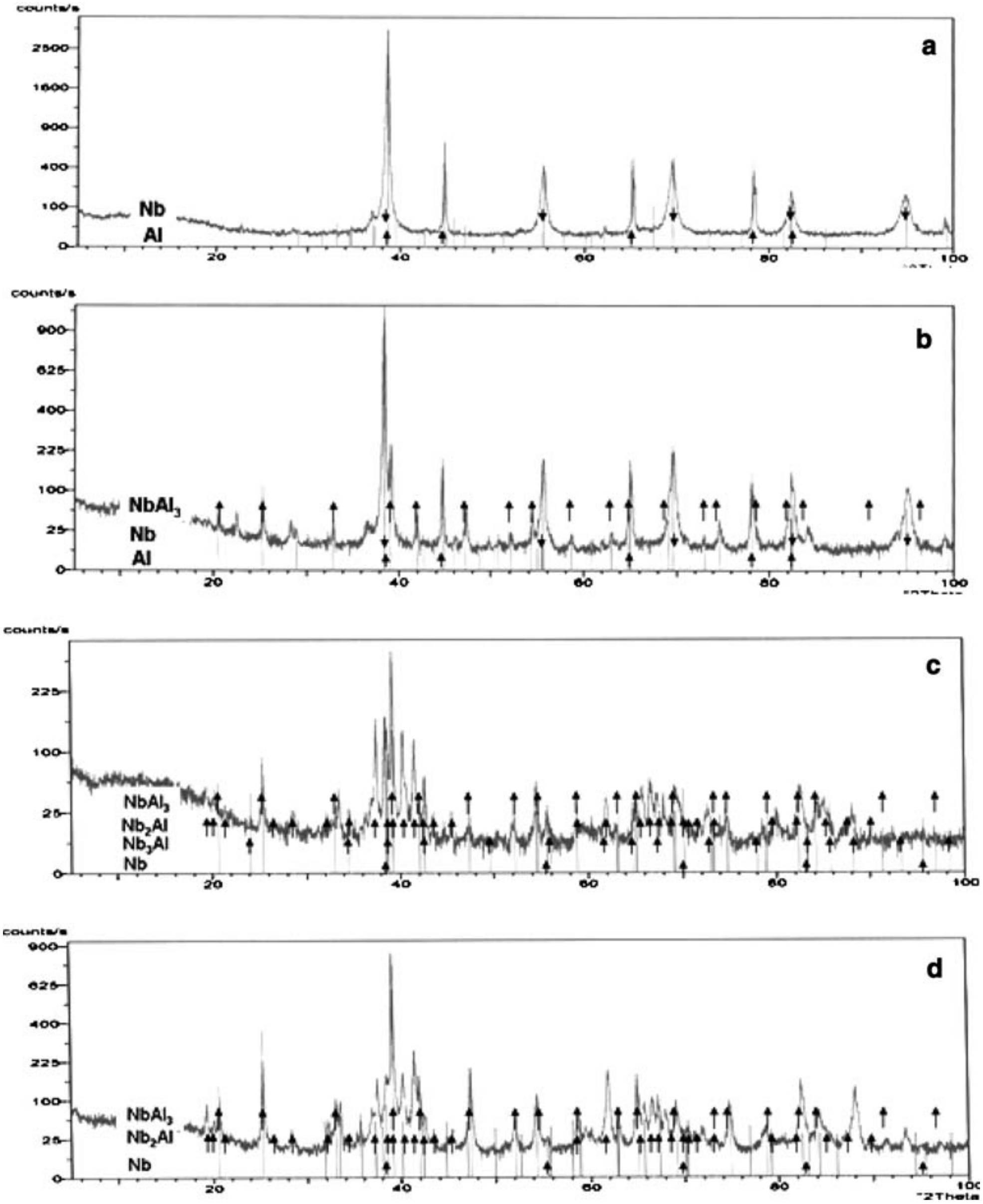

Fig. 3 XRD traces from (**a**) 3Al:1Nb sample quenched during the plateau at 660 °C, showing Al and Nb peaks; (**b**) 3Al:1Nb sample quenched after the exothermic peak showing $NbAl_3$, Al and Nb peaks; (**c**) 1Nb:1Al sample showing Nb, Nb_3Al, Nb_2Al and $NbAl_3$ peaks; (**d**) 3 Nb:2Al sample showing Nb, Nb_2Al and $NbAl_3$ peaks

The point at which there is an increase in the gradient of the exothermic peak (slightly above 900 °C) is often termed the ignition temperature [12]. In the Ni–Al system similar behaviour has been observed [14], the initial temperature rise after the melting of the aluminium was attributed to the dissolution of nickel in the liquid aluminium and the sudden increase in temperature evolution following ignition was attributed to the exothermic precipitation of the solid intermetallic phases from the liquid. In the current work the microstructures quenched from above the melting point of aluminium but prior to the ignition temperature show predominantly unreacted niobium and aluminium with a very thin layer of interfacial intermetallic whereas the samples quenched after ignition but before the peak have more complex microstructures containing eutectic mixtures and small amounts of unreacted aluminium.

Figure 4b shows the microstructure of a pellet of the same composition as Fig. 4a but quenched after the exothermic peak, the outside edge of the pellet is in the bottom left corner. Again an aluminium rich outer layer was clearly seen. There was a clear increase in the amount of intermetallic phases visible in the structure. In this sample $NbAl_3$ peaks were clearly seen on the XRD trace as well as elemental Al and Nb (Fig. 3b). Figure 4a, b shows the two microstructural regions near to the edge and in the centre of the pellets, Fig. 4c–f show the more dense central region. After the plateau at 660 °C the highly exothermic reaction begins and various niobium aluminide phases form as the pellet heats up. Figure 4c shows a pellet of 2Nb:1Al

Fig. 4 SEM micrographs of the multiphase structures formed during reaction synthesis across the Nb–Al system. (**a**) 3Al:1Nb sample quenched during the plateau at 660 °C. (**b**) 3Al:1Nb sample quenched after the exothermic peak is complete (**c**) 2Nb:1Al sample quenched from just below 1400 °C during the rapid temperature rise due to the exothermic reaction. (**d**) 2Nb:1Al sample quenched after the exothermic reaction was complete (**e**) 1Nb:1Al sample quenched after the exothermic reaction was complete and (**f**) 2Al:3Nb sample quenched after the exothermic reaction was complete

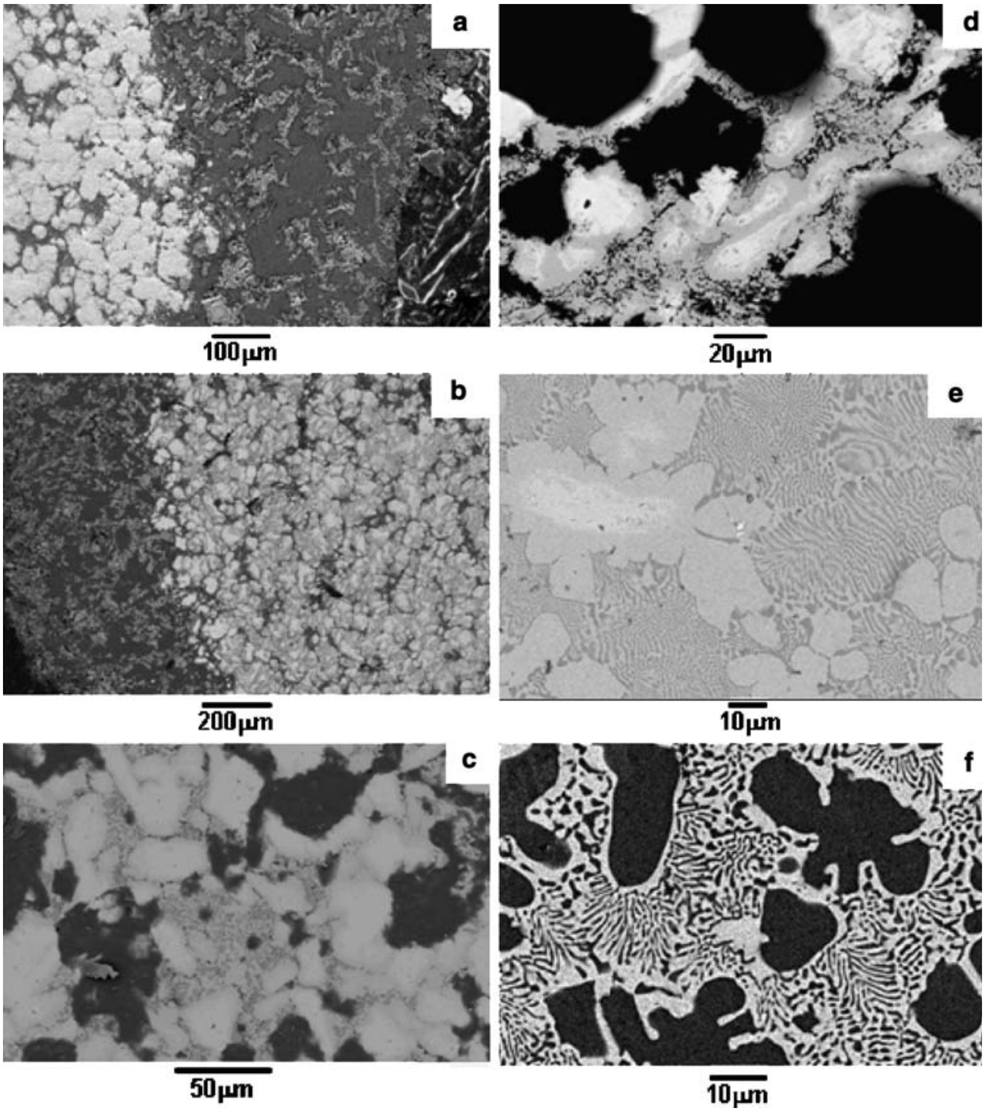

stoichiometry quenched from just below 1400 °C during the rapid temperature rise during the exothermic reaction. Nb, Nb_2Al and $NbAl_3$ were the predominant phases detected by XRD. Figure 4d shows the microstructure of a pellet of the same initial composition as Fig. 4c but quenched after the exothermic reaction is complete, again the increase in porosity and the increase in intermetallic phases formed was clear, however, the reaction did not progress to completion under these conditions. This seems to be common in reaction synthesis where intermetallic phases form prior to the exothermic reaction—it may be that these phases hinder the completion of the reaction by acting as a physical barrier to the reaction and also by reducing the heat available for the spontaneous propagation of the reaction through the sample. Finally Fig. 4e, f shows the formation of some fine scale microstructural features in pellets mixed to the stoichiometry of 1Nb:1Al and 3 Nb:2Al, respectively. XRD detected Nb, Nb_3Al, Nb_2Al and $NbAl_3$ in the sample shown in Fig. 4e and Nb, Nb_2Al and $NbAl_3$ in that shown in Fig. 4f. These XRD traces are shown in Fig. 3c, d, respectively. These multiphase structures consist only of phases with melting points above 1550 °C. Similar samples with microstructures containing ductile elemental niobium and sub-micron lamellar structures will be the subject of future mechanical property investigation by the authors. All of the reacted samples contained areas of porosity.

To conclude, the appearance of liquid aluminium during the reaction makes this system unsuitable for the simultaneous application of pressure to densify the combusting material. These results support the solid-state formation of intermetallic phases prior to the melting of aluminium. Combusted samples with initial elemental powder stoichiometries corresponding to Nb:Al and 3Nb:2Al have formed multiphase, fine scale microstructures of high melting point constituents containing a ductile elemental niobium phase.

Future work will determine the high temperature properties of these structures with the expectation that they will be potentially useful high temperature structural materials.

Acknowledgement One of the authors (I. Pong) would like to thank his parents for financial support during this work.

References

1. Hanada S (1997) Curr Opin Solid State Mater 2:279
2. Gnanamoorthy R, Hanada S (1996) Mater Sci Eng A 207:129
3. Tabaru T, Hanada S (1998) Intermetallics 6:735
4. ASM handbook http://products.asminternational.org/hbk/index.jsp. Alloy phase diagrams, Vol 3
5. Tetsui T (1999) Curr Opin Solid State Mater Sci 4:243
6. Sikka VK, Deevi SC, Viswanathan S, Swindeman RW, Santella ML (2000) Intermetallics 8:1329
7. Kamata K, Degawa T, Nagashima Y (1993) Proceedings of the first international symposium on structural intermetallics. In: Darolia R, Lewandwski JJL, Liu CT, Martin PL, Miracle DB, Nathal MV (eds) TMS, p 675
8. Dunnand DC (1994) Processing and fabrication of advanced materials III. In: Ravi VA, Srivatsan TS, Moore JJ (eds) TMS, p 771
9. Moore JJ, Feng HJ (1995) Prog Mater Sci 39:275
10. Morsi K (2001) Mater Sci Eng A 299:1
11. Minay EJ, Rawlings RD, Mcshane HB (2004) J Mater Process Technol 153–154:630
12. Gauthier V, Bernard F, Gaffet E, Josse C, Larpin JP (1999) Mater Sci Eng A272:334
13. Gauthier V, Josse C, Bernard F, Gaffet E, Larpin JP (1999) Mater Sci Eng A265:117
14. Zhu P, Li JCM, Liu CT (2002) Mater Sci Eng A329–331:57
15. Bertolino N, Monagheddu M, Tacca A, Giuliani P, Zanotti C, Tamburini UA (2003) Intermetallics 11:41
16. Dong S, Hou P, Yang H, Zou G (2002) Intermetallics 10:217
17. Minay EJ, Mcshane HB, Rawlings RD (2004) Intermetallics 12:75